Compressed Sensing: a Paradigm Shift in MRI

Christoph Forman[1]; Jens Wetzl[2]; Carmel Hayes[1]; Michaela Schmidt[1]

[1] Siemens Healthineers, Magnetic Resonance, Erlangen, Germany
[2] Pattern Recognition Lab, Friedrich-Alexander-University Erlangen-Nuremberg, Erlangen, Germany

Introduction

Reducing the complexity and length of examinations has been a major direction of research in magnetic resonance imaging (MRI) in recent years. With the introduction of the Dot engines, the complexity of MR examinations could be reduced through automatization and guidance, providing standardized and time-efficient workflows. Considerable effort has also been spent on developing methods to speed up data acquisition without degrading image quality. Accelerated imaging is a key factor to enable the visualization of rapid physiological or contrast changes in dynamic imaging. Moreover, short scans reduce the risk of artifacts due to any kind of motion during the scan. A significant speed-up of data acquisition allows both respiratory and cardiac motion to be frozen while maintaining an adequate temporal and spatial resolution. This in turn results in a high-quality and robust examination even for uncooperative patients, since data acquisition may be performed in free-breathing. Furthermore, reduced scan time and a decreased number of

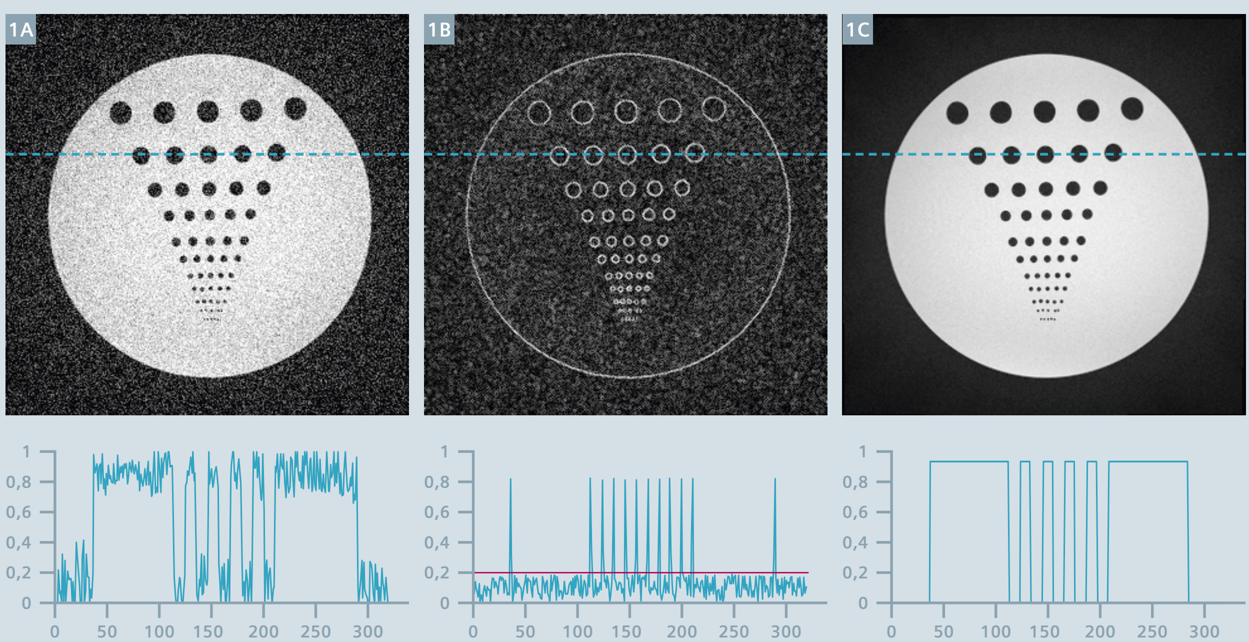

1 Additional noise reduces the homogeneity in the image of the resolution phantom **(1A)**, which can also be observed in the line plot along the dashed line. After transformation into a sparse representation using finite differences **(1B)**, the homogeneity can be restored by denoising, i.e., setting all pixels below a threshold level (red line) to 0. After the image is transformed back to its original domain, the phantom is piecewise constant **(1C)**.

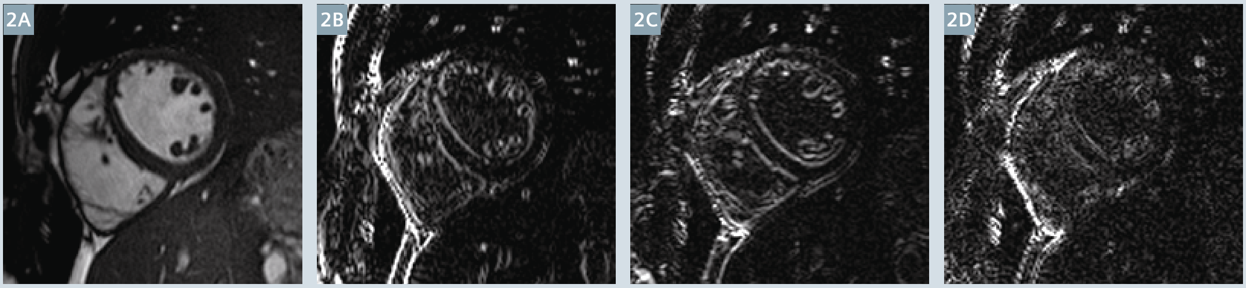

2 The short-axis view of the heart **(2A)** is transformed by the wavelet transform to achieve a sparse representation. In addition to the low-resolution representation of the original image, the wavelet transform results in three edge images **(2B-2D)**: While **(2B)** and **(2C)** contain the edges in horizontal and vertical direction, respectively, Figure 2D shows the diagonal edge components of the image. In the wavelet domain, the content of the image is sufficiently described by only few coefficients, i.e. the bright pixels.

breath-holds improve patient comfort. Last but not least, accelerated imaging means shorter examinations that can be invested in additional scans, higher resolution, or to improve the overall patient throughput. In this context, parallel imaging and compressed sensing techniques have been proposed to significantly speed up the acquisition time while maintaining diagnostic image quality.

Parallel imaging

Parallel imaging [1, 2] is well established in current clinical practice to speed up data acquisition in a large number of applications. With this technique, scan acceleration is usually achieved by uniformly sub-sampling *k*-space, for example, by skipping every other line. The resulting aliasing can be unfolded by incorporating the spatial encoding capabilities of multi-coil receiver arrays. However, the scan time reduction is often restricted to moderate acceleration factors between 2 and 4. This limitation is due to the restricted encoding capabilities in terms of number and position of the receiver coils. Additionally, acquiring less data also leads to a reduced signal-to-noise ratio (SNR).

Compressed sensing

In recent years, compressed sensing has gained large scientific attention. Originally, it was proposed as a general concept to accurately reconstruct a signal from a small number of random measurements [3, 4]. A few years later, compressed sensing[1] was introduced to MRI [5] and successfully combined with parallel imaging [6]. Exploiting the *compressibility* of medical images, this method promises to markedly exceed the acceleration rates that are feasible with parallel imaging. Although compressed sensing has denoising properties, it also has to deal with SNR loss from scan acceleration. Hence, possible acceleration factors scale with the native SNR of the scan. Up to now, the potential of compressed sensing has been shown in a large number of applications from 2D to 5D imaging [7-15].

The successful utilization of compressed sensing is a team play of data acquisition and image reconstruction. In the paper introducing compressed sensing to MRI, three criteria were identified as being essential to ensure successful image recovery from sub-sampled data [5]:

- First, the object that is acquired should have a *sparse representation* after conversion with a mathematical transformation.
- Second, *k*-space should be sub-sampled such that the aliasing results in *incoherent*, i.e. noise-like, artifacts in the image.
- Finally, image reconstruction requires a *nonlinear, iterative optimization* that simultaneously enforces a sparse representation of the resulting image. Thereby, it removes the noise-like artifacts, while it preserves its consistency to the acquired data.

These three essential requirements are discussed in detail below.

Transform sparsity

An image is considered as sparse when its informational content is represented by only a few pixels, while the contribution of the remaining majority of pixels is close to zero. In medical imaging, an angiogram provides a good example for such a sparse representation. However, in MRI, not all images are inherently sparse. But these images can also have a sparse representation utilizing a sparsifying transform. This transform provides an invertible mapping from an image to a sparse representation. Finite differences, i.e. images that contain only edge information, provide a simple technique to achieve a sparse representation, if the image is piecewise constant as shown in Figure 1. Discrete cosine transform and discrete wavelet transform are frequently used in the context of image compression, for example, in JPEG image compression. Utilizing such methods, images may be transformed into a sparse representation (see Fig. 2). In this domain, the content of the image is sufficiently described by only few coefficients,

[1] 510(k) pending. Compressed Sensing Cardiac Cine is not commercially available. Future availability cannot be guaranteed.

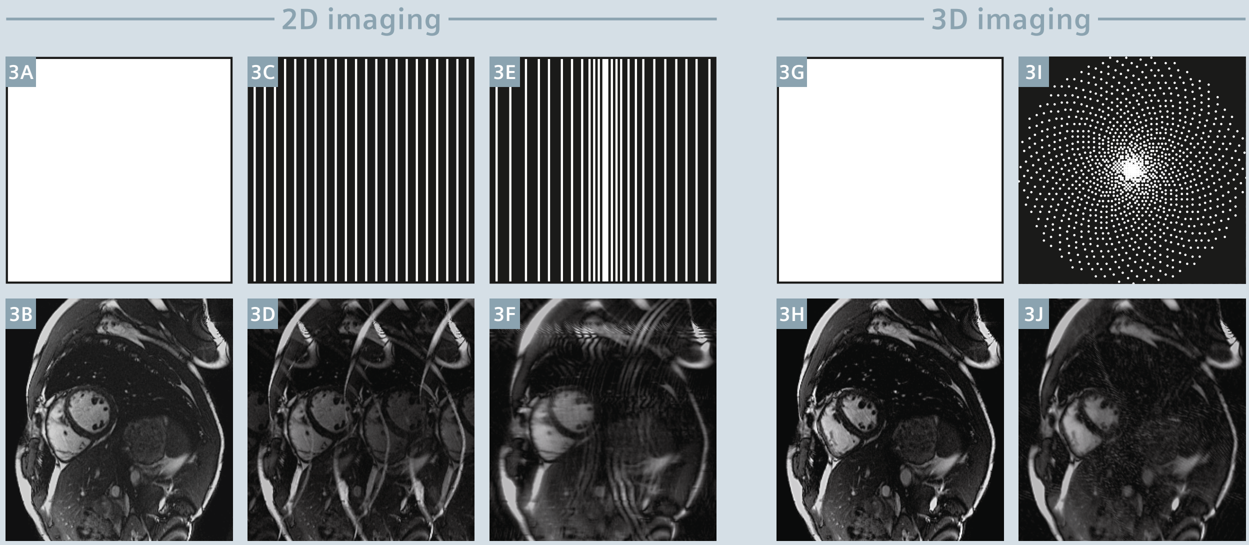

3 Examples of different sampling schemes, where *k*-space locations that are acquired are highlighted in white and the ones that are skipped are black (upper row) with corresponding image results and aliasing artifacts after Fourier transform (lower row). In 2D imaging, sub-sampling is limited to one phase-encoding direction whereas for 3D sub-sampling can be applied in two phase-encode directions. In case of CINE imaging, additional incoherence can be achieved in the temporal domain. **(3A, 3B)** Fully sampled *k*-space with artifact free result image; **(3C, 3D)** Regular subsampled *k*-space like PAT resulting in superposition of multiple ghosts; **(3E, 3F)** Irregular subsampled *k*-space as used in CS leading to incoherent aliasing artifacts similar to noise; **(3G, 3H)** Fully sampled *k*-space with artifact free result image; **(3I, 3J)** Irregular subsampled *k*-space as used in CS with noise-like artifacts.

i.e. the bright pixels. The percentage of these pixels relative to the total number of pixels defines the sparsity of the image. For image compression, pixels in this sparse representation that are below a certain threshold can be set to zero, which facilitates a compression of the signal. Once the compressed signal is converted back to its initial domain, the visual difference between the resulting image and its original version is negligible. In particular, the discrete wavelet transform has been shown to be a suitable sparsifying transform for many natural images, including MRI images, and is commonly used in compressed sensing applications. In the case of dynamic imaging, including CINE imaging, this transform can also be applied in the temporal dimension. The redundancy of information along this temporal dimension can be exploited, and often the sparsity is even higher compared to the spatial dimensions.

Incoherent sampling

Unlike the regular sub-sampling patterns used for parallel imaging, the data acquisition process for compressed sensing requires that *k*-space sub-sampling is irregular (see Fig. 3C for regular and 3E, 3I for irregular sampling). In conventional Cartesian parallel imaging, regular sub-sampling of *k*-space is advantageous in that the phase-encoding gradient is increasing linearly during the measurement, which is beneficial for physical and MRI hardware limitation reasons. However, violating the Nyquist sampling theorem in this manner results in a superposition of shifted replicas of the original signal as illustrated in Figure 3D. The number of replicas equals the chosen sub-sampling rate. This aliasing can then be unfolded utilizing the spatial encoding capabilities of the multi-coil receiver array and parallel imaging. In contrast, irregular, incoherent sub-sampling of *k*-space, as required for compressed sensing, would result in a noise-like appearance of sub-sampling artifacts (see Figs. 3F, 3J). Theoretically, completely random sub-sampling is optimal to ensure this noise-like behavior. However, purely random sampling is impractical in the case of MRI. On the one hand, large and random steps in *k*-space may require large-amplitude gradient steps and should be avoided due to hardware limitations and physical reasons. On the other hand, the sampling trajectory must be repeatable to allow the same acquisition to be reproduced with consistent image quality. Therefore, sub-sampling patterns featuring deterministic properties that mimic random sampling within the given constraints are frequently used for compressed sensing data acquisition. In 2D Cartesian imaging with pure spatial coverage, the sub-sampling is limited to one dimension, as only the phase-encoding direction is sub-sampled in MRI. But in case of 2D dynamic imaging, the sampling pattern can be varied from one time frame to the next in order to maintain sufficient incoherence for compressed sensing. In 3D Cartesian imaging, sub-sampling can be applied in two phase-encoding directions. Alternatively, non-Cartesian sampling trajectories can be used, e.g., radial or spiral imaging, that already facilitate an incoherent sampling of *k*-space for 2D imaging.

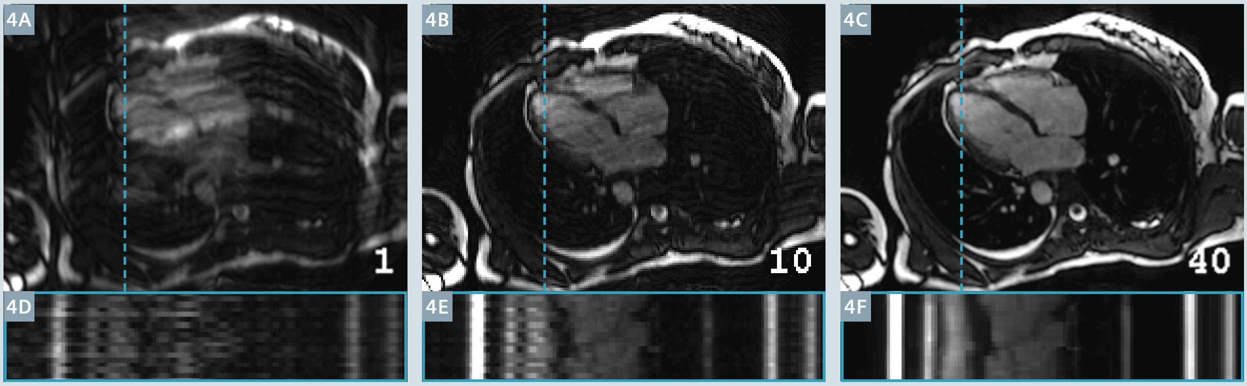

4 This Figure shows the progress of the optimization procedure to preserve data fidelity and reduce noise-like artifacts exemplarily in a Cardiac 2D CINE dataset **(4A-4C)**. While the top image shows one image of the time series, a temporal profile along the dashed line is plotted below. The incoherent sub-sampling in the spatio-temporal domain results in incoherent artifacts that dominate the image after the first iteration **(4A)**. Enforcing a sparse representation of the image and exploiting temporal redundancy, these artifacts are reduced with an increasing number of iterations **(4B)**. The compressed sensing reconstruction is terminated after 40 iterations and results in an aliasing-free image **(4C)**.

Nonlinear image reconstruction

If the two above-mentioned requirements are sufficiently met, the image can be recovered from the sub-sampled data by nonlinear, iterative reconstruction. In this reconstruction, a *data fidelity* term ensures consistency of the estimated image to the acquired data and a *transform sparsity* term enforces a sparse representation of the image in the transform domain by solving the following equation:

$$\min_x \underbrace{\|Ax-y\|_2^2}_{\text{data fidelity}} + \lambda \underbrace{\|\Phi(x)\|_1}_{\substack{\text{transform}\\ \text{sparsity}}}$$

The data fidelity term minimizes the least-squares difference ($\|\cdot\|_2^2$) between the estimated image, x, and the acquired *k*-space data, y. The system matrix, A, describes the data acquisition process, i.e., the transform from spatio-temporal to frequency domain, which is required for the comparison of the image and acquired data. Incorporating parallel imaging, it consists of the coil sensitivity maps of the individual receiver coil elements, the Fourier transform, and the applied sub-sampling pattern during data acquisition. In the transform sparsity term, the image is transformed into a sparse representation by $\Phi(\cdot)$, for example, using the discrete wavelet transform. In this term, the sum of the absolute values of the pixels in the transform domain, denoted by the ℓ_1 norm ($\|\cdot\|_1$), is minimized. Hence, the optimization procedure minimizing this equation seeks to find a solution that fulfills both criteria, data consistency and transform sparsity. This optimization procedure is more computationally intensive than conventional reconstruction, e.g., parallel imaging. The balance between data fidelity and sparsity is adjusted with the regularization parameter λ, which is usually found empirically. While small values of λ lead to an image that is closer to the acquired data, increasing this value tends to produce an image that is in favor of the sparse solution. When λ is too low, the image will be noisy, and when λ is too high a strongly filtered image appearance may be the consequence. The equation described above is iteratively minimized until a convergence criterion is met or a fixed number of iterations is reached. Figure 4 illustrates this optimization in the example of real-time CINE imaging of the heart.

Transition into clinical routine

Compressed sensing acquisition and reconstruction have been completely integrated into our clinical MRI scanners. Works-in-progress packages have been developed and tested by our clinical cooperation partners world-wide for various applications in the fields of cardiovascular [16-19], neurological [20], musculoskeletal [21-23] and oncological [24] imaging. The additional parameters needed to compose the compressed sensing protocols, for both acquisition and reconstruction, have been seamlessly integrated into our user interface (UI). A selection of possible continuous acceleration factors takes the place of discrete numbers that were familiar from parallel imaging. This facilitates a UI experience with a low level of complexity. The award-winning algorithm for compressed sensing reconstruction [8], ranking first at the ISMRM 2014 "sub-Nyquist" reconstruction challenge, has been fully integrated into the Siemens image reconstruction environment. Without the need for additional hardware, the images are directly calculated inline utilizing the full computational power of the reconstruction computer. Compressed sensing reconstruction is performed on a graphics processing unit, which provides a significant speed-up in processing time. For example, the image series of one cardiac real-time CINE slice is processed in 10 to 15 seconds.

Thanks to its high acceleration rate due to compressed sensing, real-time sequences allow for a temporal and spatial resolution comparable to that of conventional segmented acquisitions. For example, compressed sensing in cardiac imaging permits fast quantification of left-ventricular (LV) function in a single breath-hold [25]. As demonstrated in Figure 5, this sequence still provides diagnostic images for LV function quantification even in challenging scenarios, such as in the presence of arrhythmia, where conventional sequences usually fail. This sequence may also be applied in free-breathing, which is beneficial for patients who are not able to hold their breath sufficiently and, in general, allows for a simplified and more patient-friendly examination workflow.

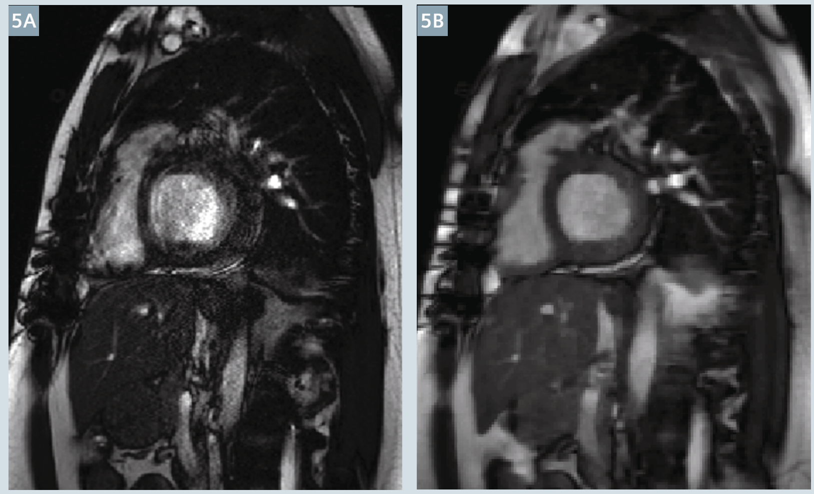

5 In cardiac imaging, the high acceleration rate due to compressed sensing enables real-time CINE imaging with a temporal and spatial resolution in a comparable range as conventional segmented acquisitions. While conventional imaging might fail in challenging scenarios, like in case of arrhythmia **(5A)**, the compressed sensing real-time sequence preserves a diagnostic image quality that still enables the quantification of LV function **(5B)**. *Images courtesy of Dr. François Pontana, Lille University Hospital, Lille, France.*

Conclusion

Compressed sensing facilitates rapid MR imaging by exploiting the fact that medical images have a sparse representation in a certain transfer domain. Representing a team play of data acquisition and image reconstruction, this allows for the reconstruction of artifact-free images following incoherent data acquisition. The acceleration enables a reduction in the acquisition time or an improvement in the spatial and/or temporal resolution. Real-time imaging featuring compressed sensing helps to reduce the need for breath-holding or ECG triggering. The integration of protocols based on compressed sensing in clinical workflows allows a significant reduction in the examination time for each patient. Our generalized integration of compressed sensing in the scanner environment will allow for the straightforward introduction of further applications that are likely to come in the near future.

References

1 M. A. Griswold, P. M. Jakob, R. M. Heidemann, M. Nittka, V. Jellus, J. Wang, B. Kiefer, and A. Haase. "Generalized Autocalibrating Partially Parallel Acquisitions (GRAPPA)". Magnetic Resonance in Medicine, Vol. 47, No. 6, pp. 1202–1210, June 2002.

2 K. Pruessmann, M. Weiger, M. B. Scheidegger, and P. Boesiger. "SENSE: Sensitivity Encoding for Fast MRI". Magnetic Resonance in Medicine, Vol. 42, No. 5, pp. 952–962, Nov. 1999.

3 D. Donoho. "Compressed Sensing". IEEE Transactions on Information Theory, Vol. 52, No. 4, pp. 1289–1306, Apr. 2006.

4 E. Candes and J. Romberg. "Sparsity and incoherence in compressive sampling". Inverse problems, Vol. 23, No. 3, pp. 969–985, Apr. 2007.

5 M. Lustig, D. Donoho, and J. M. Pauly. "Sparse MRI: The Application of Compressed Sensing for Rapid MR Imaging". Magnetic Resonance in Medicine, Vol. 58, No. 6, pp. 1182–1195, Dec. 2007.

6 D. Liang, B. Liu, J. Wang, and L. Ying. "Accelerating SENSE Using Compressed Sensing". Magnetic Resonance in Medicine, Vol. 62, No. 6, pp. 1574–1584, Dec. 2009.

7 G. Adluru, L. Chen, S. Kim, N. Burgon, E. G. Kholmovski, N. F. Marrouche, and E. V. R. DiBella. "Three-dimensional late gadolinium enhancement imaging of the left atrium with a hybrid radial acquisition and compressed sensing". Journal of Magnetic Resonance Imaging, Vol. 34, No. 6, pp. 1465-1471, Dec. 2011.

8 J. Liu, J. Rapin, T.-C. Chang, A. Lefebvre, M. O. Zenge, E. Mueller, and M. S. Nadar. "Dynamic cardiac MRI reconstruction with weighted redundant Haar wavelets". In: Proceedings of the 20th Annual Meeting of ISMRM, p. 4249, Melbourne, Australia, May 2012.

9 F. Han, S. Rapacchi, S. Kahn, I. Ayad, I. Salusky, S. Gabriel, A. Plotnik, J. P. Finn, and P. Hu, "Four-dimensional, multiphase, steady-state imaging with contrast enhancement (MUSIC) in the heart: A feasibility study in children". Magnetic Resonance in Medicine, Vol. 74, No. 4, pp. 1042-1049, Oct. 2015.

10 S. T. Ting, R. Ahmad, N. Jin, J. Craft, J. Serafim da Silveira, H. Xue, and O. P. Simonetti. "Fast Implementation for Compressive Recovery of Highly Accelerated Cardiac Cine MRI Using the Balanced Sparse Model". Magnetic Resonance in Medicine, doi: 10.1002/mrm.26224.

11 D. Stäb, T. Wech, F. A. Breuer, A. M. Weng, C. O. Ritter, D. Hahn, and H. Köstler, "High resolution myocardial first-pass perfusion imaging with extended anatomic coverage". Journal of Magnetic Resonance Imaging, Vol. 39, No. 6, pp. 1575–1587, Jun. 2014.

12 X. Chen, M. Salerno, Y. Yang, and F. H. Epstein, "Motion-compensated compressed sensing for dynamic contrast-enhanced MRI using regional spatiotemporal sparsity and region tracking: Block low-rank sparsity with motion-guidance (BLOSM)", Magnetic Resonance in Medicine, Vol. 72, No. 4, pp. 1028-1038, Oct 2014.

13 H. Xue, S. Inati, S. Sørensen, P. Kellman, and M. S. Hansen, "Distributed MRI Reconstruction Using Gadgetron-Based Cloud Computing", Magnetic Resonance in Medicine, Vol. 73, No. 3, pp. 1015-1025, March 2015.

14 J. Wetzl, F. Lugauer, M. Schmidt, A. Maier, J. Hornegger, and C. Forman. "Free-Breathing, Self-Navigated Isotropic 3-D CINE Imaging of the Whole Heart Using Cartesian Sampling", In: Proceedings of the 24th Annual Meeting of ISMRM, p. 411, Singapore, May 2016.

15 L. Feng, L. Axel, H. Chandarana, K. T. Block, D. K. Sodickson, and R. Otazo. "XD-GRASP: Golden-angle radial MRI with reconstruction of extra motion-state dimensions using compressed sensing". Magnetic Resonance in Medicine, Vol. 75, No. 2, pp. 775–788, Feb. 2016.

16 C. Forman, D. Piccini, R. Grimm, J. Hutter, J. Hornegger, and M.O. Zenge. "Reduction of respiratory motion artifacts for free-breathing whole-heart coronary MRA by weighted iterative reconstruction", Magnetic Resonance in Medicine, Vol. 73, No. 5, pp. 1885-1895, May 2015.

17 A. F. Stalder, M. Schmidt, H. H. Quick, M. Schlamann, S. Maderwald, P. Schmitt, Q. Wang, M. S. Nadar, and M. O. Zenge. "Highly undersampled contrast-enhanced MRA with iterative reconstruction: Integration in a clinical setting", Magnetic Resonance in Medicine, Vol. 74, No. 6, pp. 1652-1660, Dec. 2015

18 T. Yamamoto, K. Fujimoto, T. Okada, Y. Fushimi, A. Stalder, Y. Natsuaki, M. Schmidt, and K Togashi, "Time-of-Flight Magnetic Resonance Angiography With Sparse Undersampling and Iterative Reconstruction: Comparison With Conventional Parallel Imaging for Accelerated Imaging", Investigative Radiology, Vol. 51, No. 6, pp. 372-378, Jun 2016.

19 J. Wetzl, C. Forman, B. J. Wintersperger, L. D'Errico, M. Schmidt, B. Mailhe, A. Maier, and A. F. Stalder. "High-resolution dynamic CE-MRA of the thorax enabled by iterative TWIST reconstruction", Magnetic Resonance in Medicine, doi: 10.1002/mrm.26146.

20 E. Mussard, T. Hilbert, R. Meuli, J.-P. Thiran, and T. Kober. "Accelerated MP2RAGE Imaging Using Sparse Iterative Reconstruction", In: Proceedings of the 24th Annual Meeting of ISMRM, p. 4216, Singapore, May 2016.

21 R. Otazo, M. Nittka, M. Bruno, E. Raithel, C. Geppert, S. Gyftopoulos, M. Recht, and L. Rybak. "Sparse-SEMAC: Rapid and Improved SEMAC Metal Implant Imaging Using SPARSE-SENSE Acceleration", Magnetic Resonance Imaging, July 2016, Early View, DOI: 10.1002/mrm.26342.

22 J. Fritz, S. Ahlawat, S. Demehri, G.K. Thawait, E. Raithel, W.D. Gilson, M. Nittka. "Compressed Sensing SEMAC: 8-fold Accelerated High Resolution Metal Artifact Reduction MRI of Cobalt-Chromium Knee Arthroplasty Implants", Investigative Radiology, October 2016, Vol. 51, Issue 10, pp 666–676.

23 J. Fritz, E. Raithel, G. K. Thawait, W. Gilson, and D. F. Papp. "Six-Fold Acceleration of High-Spatial Resolution 3D SPACE MRI of the Knee Through Incoherent k-Space Undersampling and Iterative Reconstruction – First Experience". Investigative Radiology, Vol. 51, No. 6, pp. 400-409, Jun 2016.

24 D. Nickel, X. Chen, B. Mailhe, Q. Wang, Y. Son, J. M. Lee, and B. Kiefer. "Motion-resolved 3D dynamic contrast enhanced liver MRI", In: Proceedings of the 24th Annual Meeting of ISMRM, p. 4253, Singapore, May 2016.

25 G. Vincenti, P. Monney, J. Chaptinel, T. Rutz, S. Coppo, M.O. Zenge, M. Schmidt, M.S. Nadar, D. Piccini, P. Chèvre, M. Stuber, and J. Schwitter, "Compressed Sensing Single–Breath-Hold CMR for Fast Quantification of LV Function, Volumes, and Mass" JACC: Cardiovascular Imaging, Vol. 7, No. 9, pp. 882–892, Sep. 2014.

Contact

Christoph Forman
Siemens Healthcare GmbH
HC DI MR PI TIO CARD
Postbox 32 60
91050 Erlangen
Germany
christoph.forman@siemens.com

For further information, articles, case studies and keynotes on the topic of Compressed Sensing please visit

www.siemens.com/Compressed-Sensing